JACS
JOURNAL OF THE AMERICAN CHEMICAL SOCIETY
Article
Cite This: J. Am. Chem. Soc. 2019, 141, 1010−1015
pubs.acs.org/JACS

Efficient and Long-Lived Room-Temperature Organic Phosphorescence: Theoretical Descriptors for Molecular Designs

Huili Ma,[†,‡] Qian Peng,*[,§] Zhongfu An,[‡] Wei Huang,[‡] and Zhigang Shuai*[,†]

[†]Department of Chemistry and MOE Key Laboratory of Organic Optoelectronics and Molecular Engineering, Tsinghua University, 100084 Beijing, China

[§]Key Laboratory of Organic Solids and Beijing National Laboratory for Molecular Science, Institute of Chemistry, Chinese Academy of Sciences, 100190 Beijing, China

[‡]Key Laboratory of Flexible Electronics (KLOFE) and Institute of Advanced Materials (IAM), Nanjing Tech University, Nanjing 211816, China

Supporting Information

ABSTRACT: Room-temperature phosphorescence (RTP) with long afterglow from pure organic materials has attracted great attention for its potential applications in biological imaging, digital encryption, optoelectronic devices, and so on. Organic materials have been long considered to be nonphosphorescent owing to their weak molecular spin−orbit coupling and high sensitivity to temperature. However, recently, some purely organic compounds have demonstrated highly efficient RTP with long afterglow upon aggregation, while others fail. Namely, it remains a challenge to expound on the underlying mechanisms. In this study, we present the molecular descriptors to characterize the phosphorescence efficiency and lifetime. For a prototypical RTP system consisting of a carbonyl group and π-conjugated segments, the excited states can be regarded as an admixture of n → π^* (with portion α) and $\pi \rightarrow \pi^*$ (portion β). Starting from the phosphorescent process and El-Sayed rule, we deduced that (i) the intersystem crossing (ISC) rate of $S_1 \rightarrow T_n$ is mostly governed by the modification of the product of α and β and (ii) the ISC rate of $T_1 \rightarrow S_0$ is determined by the β value of T_1. Thus, the descriptors ($\gamma = \alpha \times \beta$, β) can be employed to describe the RTP character of organic molecules. From hybrid quantum mechanics and molecular mechanics (QM/MM) calculations, we illustrated the relationships among the descriptors (γ, β), phosphorescence efficiency and lifetime, and spin−orbit coupling constants. We stressed that the large γ and β values are favorable for the strong and long-lived RTP in organic materials. Experiments have reported confirmations of these molecular design rules.

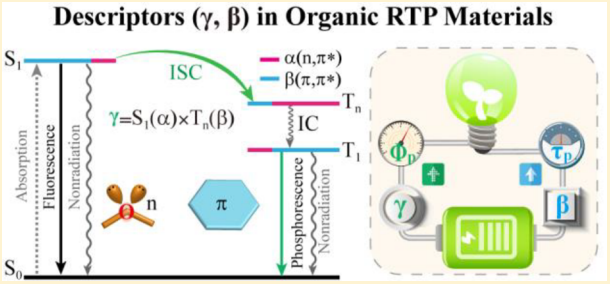

1. INTRODUCTION

More recently, room-temperature phosphorescence (RTP) from pure organic materials has attracted great attention owing to not only fundamental interests but also to application potentials in optoelectronics and biotechnologies such as organic light-emitting diodes, security systems, digital encryption, optical recording devices, sensing, and imaging.[1−9] Phosphors are conventionally limited to inorganic materials (such as rare earth ions Eu, Ce, and Pr)[10] and organometallic complex materials (Ir, Pt, etc.).[11] Pure organic phosphors with long persistent RTP are extremely rare but strongly desired for their advantages of low cost, higher processability, biocompatibility, synthetic flexibility, and appreciable stability. Having a look at the current pure organic materials, we can find that some compounds exhibit a long RTP lifetime of hundreds of milliseconds or even second order but low quantum efficiency of less than 5% in crystals,[12−14] named type I in Figure 1a, and some compounds have strong RTP but very short lifetimes of ca. 1.0 ms or microsecond order,[15] called type II in Figure 1b. In fact, the long lifetime and high quantum efficiency conflict in principle. More recently, several groups have been devoted to overcoming this challenge by designing aromatic carbonyl compounds containing n/π-groups.[16−21] However, this strategy seems invalid in some compounds because of the low Φ_p (<5%);[22−26] those are defined as type III (Figure 1c), whereas some aromatic carbonyl compounds show highly efficient and long-lived RTP and are classified as type IV (Figure 1d). Therefore, it is imperative to understand the underlying mechanism and to outline the molecular design principles for organic RTP materials.

In this article, starting from the photophysical process of phosphorescence, especially the El-Sayed rule, we introduce the molecular descriptors γ and β, related to the portion of (n, π^*) transition and (π, π^*) transition of molecular orbitals in the lowest-lying singlet and triplet excited states. Combining with the quantum mechanics/molecular mechanics (QM/MM) method, we uncover the relationship between the

Received: October 18, 2018
Published: December 19, 2018

DOI: 10.1021/jacs.8b11224
J. Am. Chem. Soc. 2019, 141, 1010−1015

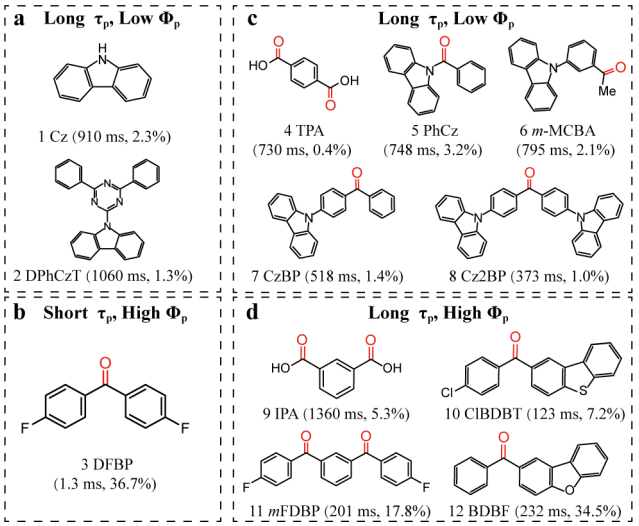

Figure 1. Chemical structures of some of the organic RTP molecules classified into four types. The phosphorescence lifetime (τ_p) and quantum yields (Φ_p) are also listed. The difference between (a) and (c) lies in the absence of carbonyl group in (a), which is very common.

molecular descriptors (γ, β) and the phosphorescence efficiency and lifetime, as well as the spin−orbit coupling constants.

2. THEORETICAL MODEL AND METHODOLOGICAL APPROACHES

2.1. Photophysical Model for Phosphorescence. As defined, phosphorescence is a radiative transition between states of different electronic spin multiplicities. For photoluminescence, the triplet state T_1 was populated by the lowest singlet state (S_1), in which the related competing photophysical processes can be clearly described by the Jablonski diagram (Figure 2a). As seen from Figure 2a, the photophysical processes occur in the following sequence: the $S_0 \rightarrow S_n$ ($n \geq 1$) light absorption; fast $S_n \rightarrow S_1$ internal conversion (IC) according to Kasha's rule; starting from S_1, the radiative decay and IC to S_0 and/or the intersystem crossing (ISC) to T_n ($n \geq 1$) with the subsequent $T_n \rightarrow T_1$ IC (the ISCs between higher-lying singlet to triplet states are neglected); finally the radiative and nonradiative decays of $T_1 \rightarrow S_0$. It is seen that the T_1 is populated through the ISC from the singlet manifold, instead of direct optical absorption. Therefore, the phosphorescence quantum yield (Φ_p) and the phosphorescence lifetime (τ_p) are expressed as

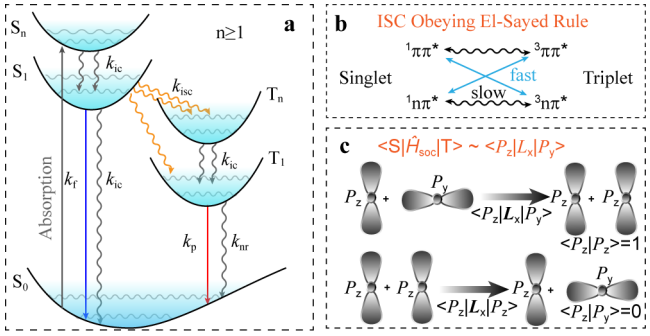

Figure 2. (a) Schematic Jablonski diagram, (b) El-Sayed's rules, and (c) the rotation property of the orbital angular momentum.

$$\Phi_p = \Phi_{isc} k_p \tau_p \quad (1)$$

$$\Phi_{isc} = k_{isc}/(k_f + k_{ic} + k_{isc}) \quad (2)$$

$$\tau_p = 1/(k_p + k_{nr}) \quad (3)$$

Here Φ_{isc} is the quantum efficiency of intersystem crossing from S_1 to T_n states. k_f and k_{ic} are the radiative and IC decay rates of $S_1 \rightarrow S_0$, respectively. k_{isc} is the ISC rate of $S_1 \rightarrow T_n$. k_p and k_{nr} represent the radiative and nonradiative decay rates of $T_1 \rightarrow S_0$, respectively. It is noted that the k_{nr} is equal to k_{isc} in the ISC of $T_1 \rightarrow S_0$, when other nonradiative deactivation channels were negligible (energy transfer, quenching by oxygen, etc.).

From eqs 1−3, two requirements can be proposed to achieve long-lived and highly efficient RTP: (i) fast ISC of $S_1 \rightarrow T_n$ ($n \geq 1$) and (ii) reduced radiative and nonradiative decay rates from T_1 to S_0. Generally, pure organic materials have small radiative decay rates ($k_p < 10^{\circ}\ s^{-1}$), slow ISC rates k_{isc} of $S_1 \rightarrow T_n$, and fast nonradiative decay rates k_{nr} of $T_1 \rightarrow S_0$ (also called ISC rate, k_{isc}).[12] Thus, the main challenges in pure organic RTP compounds are (i) enhancing the ISC process of $S_1 \rightarrow T_n$ that dominates the quantum efficiency Φ_p and (ii) suppressing the ISC rate of $T_1 \rightarrow S_0$ that determines the lifetime τ_p.

As analyzed above, faster ISC of $S_1 \rightarrow T_n$ and slower ISC of $T_1 \rightarrow S_0$ are key to guarantee high efficiency and long-lived organic phosphorescence. The ISC rate can be qualitatively estimated through El-Sayed's rules,[27] namely, the ISC rate is relatively large if the transition between S and T states involves a change of molecular orbital type (Figure 2b). For example, the transition of $^1(\pi, \pi^*) \rightarrow {}^3(n, \pi^*)$ is faster than that of $^1(\pi, \pi^*) \rightarrow {}^3(\pi, \pi^*)$ or $^1(n, \pi^*) \rightarrow {}^3(n, \pi^*)$. This is easily understood because the ISC rate is mainly determined by the spin−orbit coupling (SOC) $\langle S|\hat{H}_{SOC}|T\rangle$ and energy difference ΔE_{ST} between S and T states under the first-order perturbation and short-time approximation[28,29]

$$k_{isc} \propto |\langle S|\hat{H}_{SOC}|T\rangle|^2 \exp(-\Delta E_{ST}^2) \quad (4)$$

Within the single-electron approximation, the SOC operator is the product of the orbital and spin angular momentum. Inside an atom, the orbital angular momentum operator L always rotates the atom orbitals and changes their symmetry in real space. Namely, the operator L_x transfers the in-plane n orbital p_y to the out-of-plane π orbital p_z and vice versa (see Figure 2c), which leads to a large spatial integral between the S and T states of different orbital symmetry with respect to the molecular plane reflection.[12] The matrix element $^1\langle \pi, \pi^*|\hat{H}_{soc}|n, \pi^*\rangle^3$ or $^1\langle n, \pi^*|\hat{H}_{soc}|\pi, \pi^*\rangle^3$ is almost 2 orders of magnitude larger than $^1\langle \pi, \pi^*|\hat{H}_{soc}|\pi, \pi^*\rangle^3$ or $^1\langle n, \pi^*|\hat{H}_{soc}|n, \pi^*\rangle^3$.[30]

In organic aromatic carbonyl compounds, the excited state is the admixture of $n \rightarrow \pi^*$ and $\pi \rightarrow \pi^*$ configurations with portions α and β, respectively, where $\alpha + \beta = 1$. By this stage, the SOC between S_1 and T_n can be simplified as

$$\begin{aligned}\langle S_1|\hat{H}_{soc}|T_n\rangle &\propto {}^S\langle n + \pi|L|n + \pi\rangle^T \\ &= {}^S\langle n|L|\pi\rangle^T + {}^S\langle \pi|L|n\rangle^T + {}^S\langle n|L|n\rangle^T + {}^S\langle \pi|L|\pi\rangle^T \\ &\approx \alpha^S \times \beta^T + \beta^S \times \alpha^T = \gamma \end{aligned} \quad (5)$$

where the terms with the same n/π orbitals between S and T states vanish. γ characterizes the orbital overlap integral between S_1 and T_n states, which represents the SOC strength

DOI: 10.1021/jacs.8b11224
J. Am. Chem. Soc. 2019, 141, 1010−1015

between these two states. That is, the ISC rate of $S_1 \rightarrow T_n$ is governed by the value of γ to a large extent. As seen from eq 4, lowering the ΔE_{ST} can enhance the k_{isc}, the ISC process with the smallest ΔE_{ST} will dominate the ISC processes of $S_1 \rightarrow T_n$, and thus all the triplet states less than S_1 in energy will be considered. S_0, represented by the HOMO, in general can be characterized by the π orbital for the long-lived RTP molecules (see in Figure S1); that is, $\alpha = 0$, $\beta = 1$. Given this, the SOC between T_1 and S_0 can be expressed as

$$\langle T_l|\hat{H}_{SOC}|S_0\rangle \propto \alpha^T = 1 - \beta^T \quad (6)$$

Namely, the ISC rate of $T_1 \rightarrow S_0$ can be estimated by the α or β value of T_1. Combining eq 1 through eq 6, it is concluded that the Φ_p is primarily governed by the γ value of $S_1 \rightarrow T_n$, while the τ_p can be mainly determined by the β value of T_1. The pair of molecular descriptors (γ, β) for organic phosphorescence materials is then proposed here to evaluate the corresponding quantum yield (Φ_p) and lifetime (τ_p), which is expected to provide novel insight into the design of long-lived and efficient organic RTP materials.

2.2. Hybrid Computational Methodologies. The computational models were built by extracting a 5 × 5 × 5 cluster from the crystal structure, taking DPhCzT as an example shown in Chart 1. The combined QM/MM method

Chart 1. Setup of QM/MM Model (Taking DPhCzT as an Example)[a]

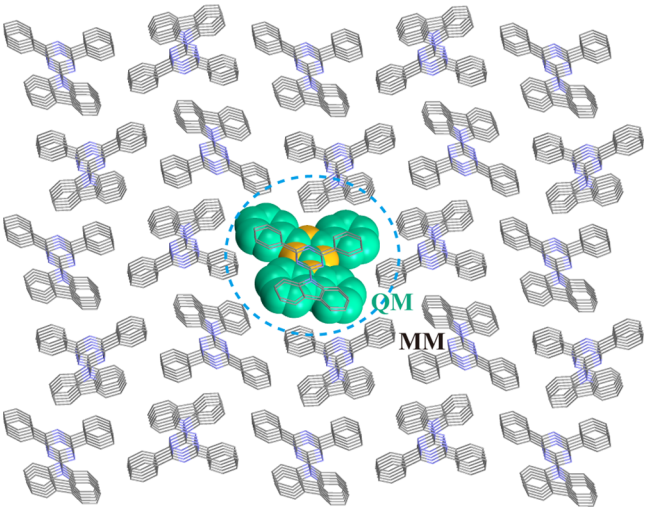

[a]The hydrogen atoms were ignored for clarity.

was used to evaluate the electronic structures of the active QM single molecule embedded in the solid state, while the surrounding molecules were defined as a rigid MM part to model the effect of the solid-state environment. The QM/MM calculations were performed by using the ChemShell 3.5[31] packages interfacing Turbomole 6.5[32] for QM and DL_POLY[33] with the general Amber force field (GAFF)[34] for the MM part. The electrostatic interaction between QM and MM is incorporated in the QM Hamiltonian (known as electrostatic embedding scheme),[35] and the van der Waals (vdW) interaction is calculated in the force-field expressions and managed by the MM code. The atomic partial charges were generated by the restrained electrostatic potential (RESP)[36] method.

All the molecules in ground states (S_0) were optimized by using the B3LYP functional together with the 6-31G(d,p) basis set, while the lowest triplet states (T_1) were obtained using unrestricted density functional theory (DFT) at the same level. Based on the T_1 geometries, we then evaluated the excitation energies of the low-lying excited states and spin−orbit couplings between singlets and triplet states at the TD-B3LYP/6-31G(d,p) level. Our previous work[37] have proved that this method can give a similar result to the CASPT2 method by taking the TPA molecule as an example. It is noted that the S_0 geometries in molecules **5** and **6** were employed due to the hugely twisted T_1 geometries. The spin−orbit couplings were carried out based on the first-order Douglas−Kroll−Hess-like spin−orbit operator derived from the exact two-component (X2C) Hamiltonian[38] by using the Beijing Density Function (BDF) program.[39−41] The γ of $S_1 \rightarrow T_n$ ($n \geq 1$) and β of T_1 states were calculated based on Mulliken population analysis of the low-lying excited states according to eqs 5 and 6, while the α was evaluated by the n-orbital that located on oxygen atom in molecules. As we analyzed above, the T_n states approaching S_1 with the smallest ΔE_{ST} should be chosen; subsequently, the $n = 6$ for molecule **9**, $n = 5$ for molecule **5**, $n = 3$ for molecule **6**, and $n = 2$ should be chosen for the remaining molecules.

3. RESULTS AND DISCUSSION

The key message we are delivering in this work is that γ of $S_1 \rightarrow T_n$ and β of T_1 in organic phosphors can be taken as the key descriptors to characterize the phosphorescence quantum yield (Φ_p) and lifetime (τ_p). To pursue the structure−property relationship, we first classified the existing organic RTP molecules from experiments into four categories (see Figure 1). Namely, the π-conjugated organic molecules with low Φ_p and long τ_p are classified as type I (Figure 1a); the aromatic ketone with high Φ_p and short τ_p as type II (Figure 1b); the aromatic carbonyl derivatives with low Φ_p and long τ_p as type III (Figure 1c); and those with high Φ_p and long τ_p as type IV (Figure 1d). Then, their excited-state electronic structures were given for the compounds in solid phase. Finally, the dependence relationships between descriptors (γ, β) and the phosphorescent efficiency and lifetime were discussed in detail, as well as the spin−orbit coupling.

3.1. Excited-State Electronic Structures and Spin−Orbit Coupling. Figure 3 shows the excited state electronic structures, including vertical excitation energies and SOCs for the compounds in solid phase, while the values of SOCs can be understood by the nature of the transition orbitals of the singlet and triplet states in Figure S2−S4. It is found that the change in ΔE_{ST} is irregular even for the same type of organic RTP molecules; for example, the values of ΔE_{ST} for $S_1 \leftrightarrow T_1$ in type III molecules (**4**−**8**) vary from 0.37 to 1.66 eV, and for $S_1 \leftrightarrow T_n$, from 0.07 to 0.73 eV ($n = 2$ for molecules **4**, **7**, and **8**; $n = 3$ for molecule **6**; $n = 5$ for molecule **5**). This indicates that it is difficult to correlate Φ_p with ΔE_{ST}. We then turn to the spin−orbit coupling coefficient between the excited singlet and triplet states, which should be essential for both τ_p and Φ_p according to eqs 1−4. Obviously, both the $\xi(S_1, T_n)$ ($n = 1, 2$) and $\xi(T_1, S_0)$ are less than 1.20 cm^{-1} in type I (molecules **1** and **2**), indicating a slow ISC process of $S_1 \rightarrow T_n$ and $T_1 \rightarrow S_0$, thus leading to the low Φ_p and long τ_p. These SOC constants in type II are enhanced by 1−2 orders of magnitude (up to ~20 cm^{-1}), which are responsible for the short τ_p and high Φ_p in molecule **3**. For type III (molecules **4**−**8**), the $\xi(S_1, T_n)$

DOI: 10.1021/jacs.8b11224
J. Am. Chem. Soc. 2019, 141, 1010−1015

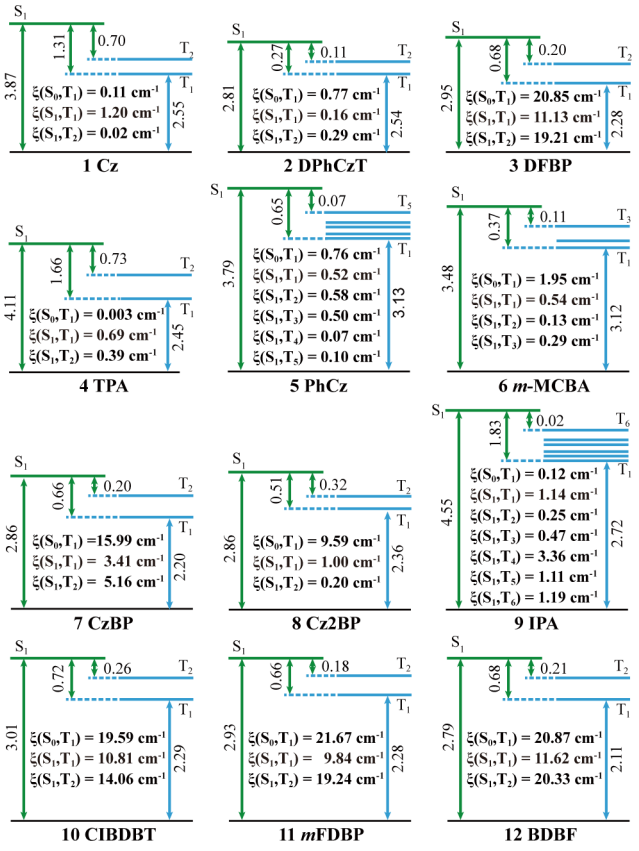

Figure 3. Energy level diagrams and SOC coefficients (ξ) for molecules **1**−**12** aggregates calculated by the QM/MM model.

values are less than 1.0 cm^{-1} except for molecule **7**, thus leading to a low Φ_p. The $\xi(T_1, S_0)$ values in molecules **4**−**8** vary from 0.003 to 15.99 cm^{-1} owing to the change in transition characters of the singlet and triplet states (see Figure S2−S4), which cause a reduced τ_p to 373 ms in molecule **8** from 795 ms in molecule **6**. When going to type IV, the $\xi(S_1, T_n)$ values are gradually increased from molecules **9** to **12**, for example, from $\xi(S_1, T_6)$ = 1.19 cm^{-1} in molecule **9** to 14.06 cm^{-1} in molecule **10**, 19.24 cm^{-1} in molecule **11**, and 20.33 cm^{-1} in molecule **12** for $\xi(S_1, T_2)$, implying an enhancement of Φ_p, up to 34.5%. Meanwhile, the increased $\xi(T_1, S_0)$ values from 0.12 to 21.67 cm^{-1} are responsible for the reduced τ_p from 1360 to 123 ms. Namely, the τ_p and Φ_p in these four types of organic RTP molecules can be qualitatively estimated through the SOC values. However, this rule sometimes cannot give a reasonably accurate estimate; for instance, the SOC values of $T_1 \rightarrow S_0$ in molecule **3** (type II) and molecules **11** and **12** (type IV) are similar (~21 cm^{-1}), whereas the τ_p is very different, with 1.3 ms in molecule **3** and ~200 ms in molecules **11** and **12**.

3.2. Molecular Descriptors for Organic Phosphorescence. As we proposed in Section 2, the phosphorescence quantum yield (Φ_p) and lifetime (τ_p) in experiment can be assessed by the simple descriptors (γ, β) in organic RTP materials. This relationship was illustrated based on the calculated γ of $S_1 \rightarrow T_n$ and β of T_1 and the experimental Φ_p and τ_p for molecules **1**−**12** in solid state in Figure 4 and Table S1. We found that the Φ_p is gradually enhanced from 0.4% to 34.5% with the increase of γ from 0.0% to 24.5%, and the exception is when the γ < 1.0%, the Φ_p fluctuates around 2.0% for types I and III (molecules **1**, **2**, and **4**−**8**); see inset in

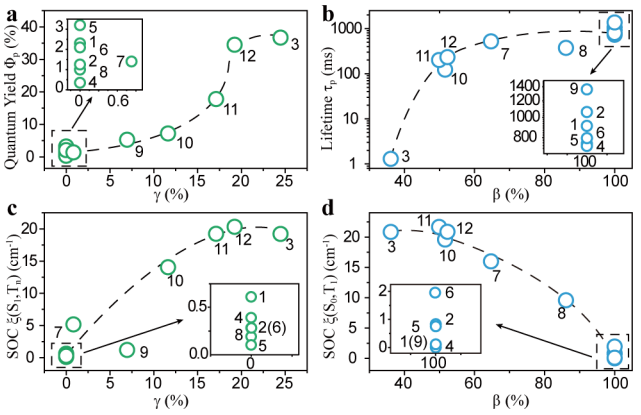

Figure 4. Dependence relationship between phosphorescence quantum yield (Φ_p), lifetime (τ_p), SOC coefficients (ξ), and the pair descriptors (γ, β). (a) Φ_p versus γ; (b) τ_p versus β; (c) $\xi(S_1, T_n)$ versus γ; (d) $\xi(T_1, S_0)$ versus β. Note that the experimental values were implemented for Φ_p and τ_p.

Figure 4a. Similarly, the lifetime τ_p is prolonged to 1360 ms from 1.3 ms when the β increases to 100.0% from 45.9%, whereas the molecules **1**, **2**, **4**−**6**, and **9** with different τ_p (from 730 to 1360 ms) have the same β value of 100.0%; see Figure 4b. These results are attributed to the fact that the large γ quickens the ISC process of $S_1 \rightarrow T_n$ to harvest triplet excitons and promotes the Φ_p (see eqs 1, 2, 4, and 5), while the large β decelerates the ISC process of $T_1 \rightarrow S_0$ and thus prolongs the τ_p (see eqs 3, 4, and 6).[17] In fact, the ISC rate is related to not only the SOC and ΔE_{ST} but also the electron-vibration coupling.[29,42] For the same γ or β within different molecules, the SOC should be identical. At this point, the electron-vibration coupling will dominate the ISC process and subsequently is responsible for the Φ_p and τ_p. This is why the same descriptors (γ, β) induce different Φ_p and τ_p; see insets in Figure 4a and b. Additionally, similar conclusions were drawn from the calculated results in the gas phase for molecules **1**−**12**; see Figure S5 and Table S2. In a word, the change in Φ_p and τ_p can be determined by the pair descriptors (γ, β) to a large extent. This makes it easily understood that the introduction of a carbonyl group (C═O) in molecules **4**−**8** (type III) is invalid to increase the Φ_p owing to the tiny γ (<1.0%). Therefore, this relationship makes it easier to expound the RTP character of organic molecules in current research.

To have a closer look at this relationship, the SOC constants for molecules **1**−**12** in aggregate phase were evaluated at the TDDFT/B3LYP/6-31G(d, p) level, and the dependence relationships between SOC constants and descriptors (γ, β) are given in Figure 4c and d, respectively. As expected from eq 5 and eq 6, the $\xi(S_1, T_n)$ is increasing with the increase of the γ value and rises by 2 orders of magnitude (from 0.10 to 20.32 cm^{-1}) when the γ goes up to ca. 20% from ca. 0%. On the contrary, the $\xi(T_1, S_0)$ is decreasing with the increase of the β value and reduces by 3 orders of magnitude as the β goes up to ca. 100% from ca. 46%. This tendency obeys the El-Sayed rule, except when the SOC constant is less than 2.0 cm^{-1}, corresponding to γ = 0.0% and β = 100.0%; see the inset in Figure 4c and 4d. Such an exception can be ascribed to two factors: (i) the descriptors (γ, β) were deduced from the SOC operator within the one-electron approximation (see eqs 5 and 6), namely, the two-electron interaction term is usually ignored, but this term will provide an important contribution

DOI: 10.1021/jacs.8b11224
J. Am. Chem. Soc. 2019, 141, 1010−1015

to the SOC value if the one-electron part is tiny; (ii) as we mentioned in Section 2, the values of descriptors (γ, β) were determined by oxygen atoms, and the small contributions from other atoms, such as nitrogen, will be non-negligible if the contribution from the oxygen atom becomes tiny. In addition, similar results were seen for molecules **1**−**12** in the gas phase; see Figure S5.

4. CONCLUSIONS

To summarize, we have proposed molecular key descriptors (γ, β) for organic RTP materials to assess the phosphorescence efficiency and lifetime. It should be noted that, in general, there exists a conflict between phosphorescence efficiency and afterglow time. Namely, the long lifetime means slow excited-state conversions and decays. Nevertheless, we find that the contradiction can be solved through molecular design independently. Starting from fundamental photophysics concepts and El-Sayed's rule for the phosphorescence process, we stressed that the molecular descriptors (γ, β) can characterize RTP for organic materials. Using the QM/MM model, we performed extensive quantum chemistry calculations for the low-lying excited state energy levels and spin−orbit coupling constants and related these with the experimental phosphorescence efficiency and lifetime. We then figure out the concomitant relationship between the descriptors (γ, β) and phosphorescence efficiency and lifetime. As expected, the organic compounds containing n/π-groups with rational molecular design are favorable for the enlargement of γ and β values, thus facilitating RTP in organic molecules with high efficiency and long-lived afterglow simultaneously.

■ ASSOCIATED CONTENT

Supporting Information

The Supporting Information is available free of charge on the ACS Publications website at DOI: 10.1021/jacs.8b11224.

Calculated HOMOs in the S_0 state for molecules **1**−**12** in the solid state and the values of γ and β between singlet and triplet states for molecules **1**−**12** in the gas and solid phases (PDF)

■ AUTHOR INFORMATION

Corresponding Authors

*qpeng@iccas.ac.cn

*zgshuai@tsinghua.edu.cn

ORCID

Huili Ma: 0000-0003-0332-2999

Qian Peng: 0000-0001-8975-8413

Zhongfu An: 0000-0002-6522-2654

Zhigang Shuai: 0000-0003-3867-2331

Notes

The authors declare no competing financial interest.

■ ACKNOWLEDGMENTS

This work is supported by the National Natural Science Foundation of China (Grant Nos. 21788102, 91622121, 21473214, 91833302, and 21875104), the Ministry of Science and Technology of China (Grant Nos. 2015CB65502 and 2017YFA0204501), Nanjing Tech Start-up Grant (Grant No. 3983500201), and the Strategic Priority Research Program of the Chinese Academy of Sciences (Grant No. XDB12020200). We are grateful to the High Performance Computing Center in Nanjing Tech University and Tsinghua University for supporting the computational resources.

■ REFERENCES

(1) Xu, S.; Chen, R.; Zheng, C.; Huang, W. Excited State Modulation for Organic Afterglow: Materials and Applications. *Adv. Mater.* **2016**, *28*, 9920.

(2) Liu, Y.; Zhan, G.; Liu, Z.; Bian, Z.; Huang, C. Room-temperature Phosphorescence from Purely Organic Materials. *Chin. Chem. Lett.* **2016**, *27*, 1231.

(3) Fateminia, S. M. A.; Mao, Z.; Xu, S.; Yang, Z.; Chi, Z.; Liu, B. Organic Nanocrystals with Bright Red Persistent Room-Temperature Phosphorescence for Biological Applications. *Angew. Chem., Int. Ed.* **2017**, *56*, 12160.

(4) Gao, R.; Yan, D. Ordered Assembly of Hybrid Room-Temperature Phosphorescence Thin Films Showing Polarized Emission and the Sensing of VOCs. *Chem. Commun.* **2017**, *53*, 5408.

(5) Hirata, S. Recent Advances in Materials with Room-Temperature Phosphorescence: Photophysics for Triplet Exciton Stabilization. *Adv. Opt. Mater.* **2017**, *5*, 1700116.

(6) Nicol, A.; Kwok, R. T. K.; Chen, C.; Zhao, W.; Chen, M.; Qu, J.; Tang, B. Z. Ultrafast Delivery of Aggregation-Induced Emission Nanoparticles and Pure Organic Phosphorescent Nanocrystals by Saponin Encapsulation. *J. Am. Chem. Soc.* **2017**, *139*, 14792.

(7) Zhen, X.; Tao, Y.; An, Z.; Chen, P.; Xu, C.; Chen, R.; Huang, W.; Pu, K. Ultralong Phosphorescence of Water-Soluble Organic Nanoparticles for In Vivo Afterglow Imaging. *Adv. Mater.* **2017**, *29*, 1606665.

(8) Kabe, R.; Adachi, C. Organic Long Persistent Luminescence. *Nature* **2017**, *550*, 384.

(9) Wang, J.; Gu, X.; Ma, H.; Peng, Q.; Huang, X.; Zheng, X.; Sung, S. H. P.; Shan, G.; Lam, J. W. Y.; Shuai, Z.; Tang, B. Z. A Facile Strategy for Realizing Room Temperature Phosphorescence and Single Molecule White Light Emission. *Nat. Commun.* **2018**, *9*, 2963.

(10) Li, Y.; Gecevicius, M.; Qiu, J. Long Persistent Phosphors-from Fundamentals to Applications. *Chem. Soc. Rev.* **2016**, *45*, 2090.

(11) Yam, V. W.-W.; Au, V. K.-M.; Leung, S. Y.-L. Light-Emitting Self-Assembled Materials Based on d^8 and d^{10} Transition Metal Complexes. *Chem. Rev.* **2015**, *115*, 7589.

(12) Turro, N. J.; Ramamurthy, V.; Scaiano, J. C. *Modern Molecular Photochemistry of Organic Molecules*, 1st ed.; University Science Books: Sausalito, CA, 2010.

(13) An, Z.; Zheng, C.; Tao, Y.; Chen, R.; Shi, H.; Chen, T.; Wang, Z.; Li, H.; Deng, R.; Liu, X.; Huang, W. Stabilizing Triplet Excited States for Ultralong Organic Phosphorescence. *Nat. Mater.* **2015**, *14*, 685.

(14) Sun, C.; Ran, X.; Wang, X.; Cheng, Z.; Wu, Q.; Cai, S.; Gu, L.; Gan, N.; Shi, H.; An, Z.; Shi, H.; Huang, W. Twisted Molecular Structure on Tuning Ultralong Organic Phosphorescence. *J. Phys. Chem. Lett.* **2018**, *9*, 335.

(15) Yuan, W. Z.; Shen, X. Y.; Zhao, H.; Lam, J. W. Y.; Tang, L.; Lu, P.; Wang, C.; Liu, Y.; Wang, Z.; Zheng, Q.; Sun, J. Z.; Ma, Y.; Tang, B. Z. Crystallization-Induced Phosphorescence of Pure Organic Luminogens at Room Temperature. *J. Phys. Chem. C* **2010**, *114*, 6090.

(16) Bolton, O.; Lee, K.; Kim, H.-J.; Lin, K. Y.; Kim, J. Activating Efficient Phosphorescence from Purely Organic Materials by Crystal Design. *Nat. Chem.* **2011**, *3*, 205.

(17) Zhao, W.; He, Z.; Lam, J. W. Y.; Peng, Q.; Ma, H.; Shuai, Z.; Bai, G.; Hao, J.; Tang, B. Z. Rational Molecular Design for Achieving Persistent and Efficient Pure Organic Room-Temperature Phosphorescence. *Chem.* **2016**, *1*, 592.

(18) He, Z.; Zhao, W.; Lam, J. W. Y.; Peng, Q.; Ma, H.; Liang, G.; Shuai, Z.; Tang, B. Z. White Light Emission from a Single Organic Molecule with Dual Phosphorescence at Room Temperature. *Nat. Commun.* **2017**, *8*, 416.

(19) Bian, L.; Shi, H.; Wang, X.; Ling, K.; Ma, H.; Li, M.; Cheng, Z.; Ma, C.; Cai, S.; Wu, Q.; Gan, N.; Xu, X.; An, Z.; Huang, W.

Simultaneously Enhancing Efficiency and Lifetime of Ultralong Organic Phosphorescence Materials by Molecular Self-Assembly. *J. Am. Chem. Soc.* **2018**, *140*, 10734.
(20) Zhang, X.; Xie, T.; Cui, M.; Yang, L.; Sun, X.; Jiang, J.; Zhang, G. General Design Strategy for Aromatic Ketone-Based Single-Component Dual-Emissive Materials. *ACS Appl. Mater. Interfaces* **2014**, *6*, 2279.
(21) Wang, T.; Tang, Z.; Xu, D.; Sun, W.; Deng, Y.; Wang, Q.; Zhang, X.; Su, P.; Zhang, G. Waterborne Polyacrylates with Thermally Activated Delayed Fluorescence and Two-State Phosphorescence. *Mater. Chem. Front.* **2018**, *2*, 559.
(22) Gong, Y.; Chen, G.; Peng, Q.; Yuan, W. Z.; Xie, Y.; Li, S.; Zhang, Y.; Tang, B. Z. Achieving Persistent Room Temperature Phosphorescence and Remarkable Mechanochromism from Pure Organic Luminogens. *Adv. Mater.* **2015**, *27*, 6195.
(23) Li, C.; Tang, X.; Zhang, L.; Li, C.; Liu, Z.; Bo, Z.; Dong, Y. Q.; Tian, Y.-H.; Dong, Y.; Tang, B. Z. Reversible Luminescence Switching of an Organic Solid: Controllable On-Off Persistent Room Temperature Phosphorescence and Stimulated Multiple Fluorescence Conversion. *Adv. Opt. Mater.* **2015**, *3*, 1184.
(24) Yang, Z.; Mao, Z.; Zhang, X.; Ou, D.; Mu, Y.; Zhang, Y.; Zhao, C.; Liu, S.; Chi, Z.; Xu, J.; Wu, Y.-C.; Lu, P.-Y.; Lien, A.; Bryce, M. R. Intermolecular Electronic Coupling of Organic Units for Efficient Persistent Room-Temperature Phosphorescence. *Angew. Chem., Int. Ed.* **2016**, *55*, 2181.
(25) Xie, Y.; Ge, Y.; Peng, Q.; Li, C.; Li, Q.; Li, Z. How the Molecular Packing Affects the Room Temperature Phosphorescence in Pure Organic Compounds: Ingenious Molecular Design, Detailed Crystal Analysis, and Rational Theoretical Calculations. *Adv. Mater.* **2017**, *29*, 1606829.
(26) Xiong, Y.; Zhao, Z.; Zhao, W.; Ma, H.; Peng, Q.; He, Z.; Zhang, X.; Chen, Y.; He, X.; Lam, J. W. Y.; Tang, B. Z. Designing Efficient and Ultralong Pure Organic Room-Temperature Phosphorescent Materials by Structural Isomerism. *Angew. Chem., Int. Ed.* **2018**, *57*, 7997.
(27) El-Sayed, M. A. Triplet State. Its Radiative and Nonradiative Properties. *Acc. Chem. Res.* **1968**, *1*, 8.
(28) Shuai, Z.; Peng, Q. Excited States Structure and Processes: Understanding Organic Light-Emitting Diodes at the Molecular Level. *Phys. Rep.* **2014**, *537*, 123.
(29) Shuai, Z.; Peng, Q. Organic Light-Emitting Diodes: Theoretical Understanding of Highly Efficient Materials and Development of Computational Methodology. *Natl. Sci. Rev.* **2016**, *4*, 224.
(30) Gao, X.; Bai, S.; Fazzi, D.; Niehaus, T.; Barbatti, M.; Thiel, W. Evaluation of Spin-Orbit Couplings with Linear-Response Time-Dependent Density Functional Methods. *J. Chem. Theory Comput.* **2017**, *13*, 515.
(31) Sherwood, P.; de Vries, A. H.; Guest, M. F.; Schreckenbach, G.; Catlow, C. R. A.; French, S. A.; Sokol, A. A.; Bromley, S. T.; Thiel, W.; Turner, A. J.; Billeter, S.; Terstegen, F.; Thiel, S.; Kendrick, J.; Rogers, S. C.; Casci, J.; Watson, M.; King, F.; Karlsen, E.; Sjøvoll, M.; Fahmi, A.; Schäfer, A.; Lennartz, C. QUASI: A General Purpose Implementation of the QM/MM Approach and Its Application to Problems in Catalysis. *J. Mol. Struct.: THEOCHEM* **2003**, *632*, 1.
(32) Ahlrichs, R.; Bär, M.; Häser, M.; Horn, H.; Kölmel, C. Electronic Structure Calculations on Workstation Computers: The Program System Turbomole. *Chem. Phys. Lett.* **1989**, *162*, 165.
(33) Smith, W.; Forester, T. R. DL_POLY_2.0: A General-Purpose Parallel Molecular Dynamics Simulation Package. *J. Mol. Graphics* **1996**, *14*, 136.
(34) Wang, J.; Wolf, R. M.; Caldwell, J. W.; Kollman, P. A.; Case, D. A. Development and Testing of a General Amber Force Field. *J. Comput. Chem.* **2004**, *25*, 1157.
(35) Bakowies, D.; Thiel, W. Hybrid Models for Combined Quantum Mechanical and Molecular Mechanical Approaches. *J. Phys. Chem.* **1996**, *100*, 10580.
(36) Bayly, C. I.; Cieplak, P.; Cornell, W.; Kollman, P. A. A Well-Behaved Electrostatic Potential Based Method Using Charge Restraints for Deriving Atomic Charges: the RESP Model. *J. Phys. Chem.* **1993**, *97*, 10269.
(37) Ma, H.; Shi, W.; Ren, J.; Li, W.; Peng, Q.; Shuai, Z. Electrostatic Interaction-Induced Room-Temperature Phosphorescence in Pure Organic Molecules from QM/MM Calculations. *J. Phys. Chem. Lett.* **2016**, *7*, 2893.
(38) Li, Z.; Xiao, Y.; Liu, W. On the Spin Separation of Algebraic Two-Component Relativistic Hamiltonians. *J. Chem. Phys.* **2012**, *137*, 154114.
(39) Li, Z.; Suo, B.; Zhang, Y.; Xiao, Y.; Liu, W. Combining Spin-Adapted Open-Shell TD-DFT with Spin-Orbit Coupling. *Mol. Phys.* **2013**, *111*, 3741.
(40) Liu, W.; Hong, G.; Dai, D.; Li, L.; Dolg, M. The Beijing Four-Component Density Functional Program Package (BDF) and Its Application to EuO, EuS, YbO and YbS. *Theor. Chem. Acc.* **1997**, *96*, 75.
(41) Liu, W.; Wang, F.; Li, L. The Beijing Density Functional (BDF) Program Package: Methodologies and Applications. *J. Theor. Comput. Chem.* **2003**, *02*, 257.
(42) Peng, Q.; Niu, Y.; Shi, Q.; Gao, X.; Shuai, Z. Correlation Function Formalism for Triplet Excited State Decay: Combined Spin-Orbit and Nonadiabatic Couplings. *J. Chem. Theory Comput.* **2013**, *9*, 1132.

DOI: 10.1021/jacs.8b11224
J. Am. Chem. Soc. 2019, 141, 1010−1015